Research Article

Journal of PeptideScience

Received: 14 December 2009 Revised: 5 March 2010 Accepted: 19 March 2010 Published online in Wiley Interscience: 27 May 2010

(www.interscience.com) DOI 10.1002/psc.1241

Improved therapeutic responses for liposomal doxorubicin targeted via thrombospondin peptidomimetics versus untargeted doxorubicin

M. P. Rivera-Fillat,[a] F. Reig,[b]* E. M. Martínez[a] and M. R. Grau-Oliete[a]

New therapies in cancer treatment are focusing on multifaceted approaches to starve and kill tumors utilizing both antiangiogenic and chemotherapeutic compounds. In this work, we searched for a peptide vector that would home liposomes both to endothelial and tumor cells. [Abu6]TSPB and [Abu6]TSPA, aspartimide analogs of natural sequences of TSP-1 and TSP-2, respectively, were tested for adhesion of tumor and endothelial cells, *in vivo* and *in vitro* antiangiogenic effects, and *in vivo* antitumor action. Both peptides support the adhesion of both types of cells, but only [Abu6]TSPA inhibits the angiogenesis *in vivo*, and [Abu6]TSPA-targeted L-DOX decreases by 58% ($P < 0.008$) the HT29 tumor growth in nude mice. The improvement in the doxorubicin antitumor effect should be attributed to the antiangiogenic effect of [Abu6]TSPA, since [Abu6]TSPB, despite being a good ligand for both cell types, had no effect on tumor growth. Copyright © 2010 European Peptide Society and John Wiley & Sons, Ltd.

Keywords: targeting; liposomal doxorubicin; thrombospondin; peptide analogs; angiogenesis

Introduction

Solid tumors recruit new blood vessels to support their specific growth, and epitopes expressed on endothelial cells can function as targets for the chemo-antiangiogenic therapy of cancer. It is well established that the associated endothelial cells proliferate during chronic angiogenesis in tumors, albeit at lower frequencies than the tumor cells themselves [1,2]. Apparently, because of the lower rate of cell division, replication of these endothelial cells is only weakly disrupted by the episodic regimens of standard chemotherapeutic protocols. Targeted liposomes have been used for the specific delivery of drugs to blood vessels [3–5], demonstrating that antitumor effects of chemotherapeutic cytotoxic drugs can be augmented when they are combined with antiangiogenic inhibitors.

One of the first naturally occurring inhibitors of angiogenesis to be discovered was TSP-1 and the highly related protein TSP-2. Different cellular receptors that recognize specific peptide domains of TSP-1 have been identified both in tumor and endothelial cells, and they appear to mediate a variety of biological functions [6]. Sequences from the TSRs reportedly contain antiangiogenic activity [7,8] such as the KRFKQDGGWSHW sequence, which consists of a WSHW motif that binds to latent TGF-β and KRFK, at the boundary between the first and second TSR, implicated in the TGF-β activation [9]. Similarly, TSP-2 also contains the WSHW motif, but it has TRIR instead of the KRFK sequence, which means that it binds but does not activate TGF-β [10]. Systemic injection of peptides that contain or lack the RFK sequence inhibits tumor growth and their activity is dependent upon an L- to D-amino acid racemization [11].

Based on those observations, in this work, we searched for a peptide vector that would home the liposomes both to endothelial and tumor cells. To this end, we selected two peptides from the TSRs of TSP-1 and TSP-2: [Abu6]TSPB and [Abu6]TSPA that are aspartimide analogs of the natural motives KRFKQDGGWSHW (TSP_1-B) and TRIRQDGGWSHW (TSP_2-A), respectively [12,13]. We assessed their capacity for binding tumor and endothelial cells, their effect on the proliferation of both cell types, and their effects on angiogenesis both *in vitro* (tube formation) and *in vivo* (CAM). Finally, the antitumor activity of peptide vector L-DOX was measured on a subcutaneous HT29 colon carcinoma model, comparing this activity with that of free doxorubicin (DOX) and untargeted L-DOX.

* *Correspondence to: F. Reig, Group of Peptide Chemistry, Department of Nanotechnology, IQAC, CSIC, Jordi Girona Salgado, 18-26, 08034 Barcelona, Spain. E-mail: fripfr@iqac.csic.es*

a *Pathology and Experimental Therapeutics Group, CSIC-ICCC, Barcelona, Spain*

b *Group of Peptide Chemistry, Department of Nanotechnology, IQAC, CSIC, Barcelona, Spain*

Abbreviations used: *[Abu6]TSPB, aspartimide analog of TSP_1-B; [Abu6]TSPA, aspartimide analog of TSP_2-A; CAM, chick chorio-allantoic membrane; Chol, cholesterol; DPPE, dipalmitoyl phosphatidyl ethanolamine; ECGS, endothelial cell-growth supplement; FGF-b, basic fibroblast growth factor; HPC, hydrogenated phosphatidyl choline; HUVEC, human umbilical vein endothelial cell; L-DOX, liposomal doxorubicin; NGPE, N-glutaryl–phospatidyl ethanolamine; PG, phosphatidyl glycerol; S-NHS, N-hydroxysulfosuccinimide; TGF-β, transforming growth factor beta; TSRs, type 1 repeats; TSP-1, thrombospondin 1; TSP-2, thrombospondin 2; TSP_1-B, peptide sequence of TSP-1; TSP_2-A, peptide sequence of TSP-2.*

Materials and Methods

Chemicals

HPC was provided by the Asahi Chemical Industry Co. Ltd. (Tokyo, Japan). PG, DPPE, and Chol were obtained from Sigma (St. Louis, MO, USA). Lipids were dissolved in chloroform/methanol and stored at −20 °C until use. Glutaric anhydride, EDC, and S-NHS were from Fluka (Hannover, Germany). Doxorubicin hydrochloride was purchased from Tedec-Meiji Farma S. A. (Alcalá de Henares, Spain). Solvents used to prepare liposomes, chloroform, and methanol as well as salts used to prepare buffers were supplied by Merck (Darmstadt, Germany) reagent grade. NGPE was synthesized in our laboratory following the description given in [14]. Lipocroman^R included in the liposomal composition was a gift from Lipotec (Barcelona, Spain). Dialysis membranes were Spectra-por MWCO 14 000.

Peptides corresponding to the sequences of the TSRs of thrombospondin, TSP_1-B and TSP_2-A, and their aspartimide analogs, [Abu6]TSPB and [Abu6]TSPA, were synthesized in the Peptides Department of IIQAB-CSIC in Barcelona. Details of the synthesis and physicochemical characterization are given in Refs [12,13]. Crude peptides were purified by preparative HPLC and controlled by amino acid analysis and MS.

Cells and Media

HT29 human colon carcinoma cells were cultured in 25-cm^2 flasks (Costar, Corning, NY, USA) in McCoy medium (GibcoBRL, Grand Island, NY, USA), supplemented with 10% fetal calf serum (FCS; Biological Industries, Beit Haemek, Israel) at 37 °C in a humidified atmosphere of 5% CO_2. HUVE cells (Department of Cell Biology, University of Barcelona, Spain) were maintained on gelatin-coated plates in M199 medium (Sigma-Aldrich Chemical Co., Barcelona, Spain) with 20% FCS and 1% ECGS (Sigma-Aldrich Chemical Co.) in a humidified atmosphere of 5% CO_2 at 37 °C. For experiments, HUVECs were grown to confluence and used between passages 4 and 7.

Preparation of Liposomes

Liposomes composed of HPC/PG/Chol/$^{\#}$ NGPE (24%, 18%, 44%, and 10% molar, respectively) contained 4% Lipocroman^R, a vitamin E-derived antioxidant that stabilizes and prolongs the liposome half-life in blood [15]. $^{\#}$ NGPE is a PE derivative with a carboxy terminal group used for binding peptides or proteins to the lipid bilayer surface. PG was included to provide a negative charge to the vesicles that would improve entrapment of cationic DOX [16].

Small uni- and multilamellar vesicles (size <200 nm) were prepared under sterile conditions by a combination of standard methods of thin-film formation, hydration, and sonication.

Two batches of vesicles were prepared in parallel, one with DOX and the other without. Lipid films containing 520 µmols of total lipids were prepared by elimination of solvent in a rotary evaporator followed by 1 h of connection to a vacuum pump. All the processes were carried out at 60 °C, because the transition temperature of HPC determined by differential scanning calorimetry was around 53 °C. Films were hydrated with 9 ml of 10% sterile sucrose, using gentle agitation (30 s, six times) to detach lipids from vessel wall, followed by addition of either 9 ml of 10% sucrose or 9 ml of DOX in 10% sucrose (5 mg/ml). Both samples were submitted to ten cycles of agitation (1 min) and incubation (10 min) in order to favor the entrapment of DOX. Size reduction was achieved after sonication with a titanium tip (13-mm diameter). Usually eight times were enough to achieve diameters in the range 120–150 nm. To eliminate Ti probe residues and lipid aggregates, liposomes were centrifuged at 3000*g* for 20 min. Although physicochemical studies indicated that liposomal preparations were stable as far as size and DOX entrapment were concerned, liposomes were prepared just before use in all experiments.

Preparation of Peptide–Liposome Conjugates

Carboxylic groups of NGPE exposed on the surface of liposomes were activated as follows: 9 ml of liposomes either empty or loaded with DOX was incubated with a mixture of 126 mg of EDC and 75 mg of S-NHS (dissolved in 1 ml of water) for 15 min at room temperature. Thereafter, the reaction medium was taken to pH 7.5–8 with 1 N NaOH (*ca* 215 µl), and 41 mg of peptide dissolved in 500 µl of borate buffer, pH 7.5, was added. The reaction mixture was gently homogenized and left overnight at 4 °C. Excess of reactants, nonentrapped DOX, and nonlinked peptide were eliminated by dialysis of the liposomal samples against 10% sucrose.

Liposomes were characterized quantifying DOX by fluorescence (480/550 nm), phospholipid by inorganic phosphate analysis (atomic absorption), and peptide by amino acid analysis using Nle as the internal standard. Vesicle size was determined in Malvern autosizer. All preparations had diameters under 200 nm and the main characteristics were: DOX/phospholipid = 0.21–0.26 mg/µmol and peptide/phospholipid = 0.03–0.04 mg/µmol.

Adhesion Assays

Black 96-well plates with a flat clear bottom (Costar) were coated with 50 µl increasing concentrations of peptides (0.2–100 µg/well) or 20 µg/ml of recombinant human TSP-1 (Calbiochem, San Diego, CA, USA) in phosphate-buffered saline (PBS) by overnight incubation at 4 °C and blocked with 1% BSA (Boheringer Mannheim, Mannheim, Germany) for 1 h after washing. Cells suspended in serum-free RPMI without phenol red (GibcoBRL, Barcelona, Spain) were plated in each coated well at 3×10^3/100 µl. The plate was incubated for 2 h (37 °C in a humidified atmosphere of 5% CO_2) and after washing (2×) with PBS, 100 µl of 5 µM Calcein-AM (Molecular Probes, Leiden, The Netherlands) in RPMI were added to each well and incubated for 45 min (37 °C, 5% CO_2). Free Calcein-AM was removed by careful washing (3×) with RPMI and fluorescence (485/535 filters) was measured in a microtiter plate reader (1420 VICTOR^2 EG&G Wallac, Turku, Finland) after adding 100 µl of RPMI medium. Background fluorescence was measured in a duplicate set of BSA-blocked uncoated wells. The cell adhesion was calculated as a percentage of corrected (background subtracted) fluorescence of peptide-coated wells with respect to that measured in TSP-1-coated wells.

Cell Proliferation

HT29 cell proliferation was measured by a sulforhodamine (SRB)-based colorimetric method [17]. Briefly, 190 µl of HT29 cells suspended at 1.5×10^4 cells/ml in culture medium was plated in each well of 96-well flat-bottomed microtiter plates (Costar) and

Journal of PeptideScience

allowed to attach for 24 h. Next, 10 µl of peptide serial dilutions (*T*, test wells) or excipient [*C*, control (CTR) wells] was added to the respective wells. Parallel cultures were fixed with 10% trichloroacetic acid (TCA) (see below) for measuring the T_0 value. After 72-h incubation at 37 °C in a humidified atmosphere of 5% CO_2, the cells were fixed with TCA (10% final concentration) and stained with SRB. OD was measured (490 nm) in a microtiter plate reader (1420 VICTOR^2, EG&G Wallac, Turku, Finland) and corrected OD (background subtracted) was used to calculate the proliferation as: $T - T_0/C - T_0 \times 100$.

HUVEC proliferation was measured on cells cultured in M199 medium supplemented with 1% ECGS, 1% heparin, and 20% FBS. Cells, lifted with 0.05% trypsin-EDTA and resuspended at 1.5×10^5 cells/ml in culture medium were plated (190 µl/well) on 96-well black flat-bottomed culture plates' clear bottom (Costar), previously coated with 1% gelatin, and allowed to attach for 24 h. Peptides were then added to each well at increasing concentrations (10 µl) and the cells were cultured for 72 h at 37 °C in a humidified atmosphere of 5% CO_2. Finally, after removing the medium, 200 µl of 2 µM Calcein-AM in PBS was added and the fluorescence was measured (485/535 filters) after incubation for 45 min. Proliferation of peptide-treated cultures was expressed as the percentage of CTRs (excipient treated).

Tube Formation Assay

Early passages of HUVECs in M199 medium containing 10% FBS were grown on 50 µl of Matrigel (Becton Dickinson, San Jose, CA, USA) on flat-bottomed 96-well plates (Costar) at 7×10^4 cells/well (100 µl). After adding the reagents, cells were incubated in an atmosphere of 5% CO_2 at 37 °C for 24 h. Sprouting and tubulogenesis were observed under an inverted phase-contrast microscope and photographed. Images were scanned and tube length was measured using Scion Image software (Scion Corp., Frederich, MD, USA).

Angiogenesis in CAM

Fertilized chicken eggs (Gibert, Barcelona, Spain) were used at day 10 of development. After extraction of 2–3 ml of ovalbumin with a sterile syringe, a window (1 cm^2) was opened allowing direct access to underlying CAM. Peptides previously coated (5 µl, 0.2 mg/ml) on 13-mm diameter sterile plastic membranes (Thermanox, Nalgene, NUNC International) were applied to the top of CAM. Uncoated membranes and membranes coated with 5 µl of FGF-b (10 ng/µl) were used as CTRs. Windows were covered with sterile cellophane and embryos incubated for 48 h at 38 °C with 60% humidity. Digital images of the CAM were captured using a binocular dissection microscope (Leica MZ8, Heerbrugg, Switzerland) and a color charge-coupled device video camera (Sony Model DXC-950, Sony Corporation, Tokyo, Japan) and saved as *.tif files. Areas containing only capillary plexus were selected for quantification and at least four and up to ten such areas per micrograph were identified. Angiogenesis quantification was done with Scion Image software measuring the number of branched vessels per area.

Tumor Growth

Five-week-old male nu/nu Swiss mice weighing ~23 g (Iffa-Credo, Barcelona, Spain) were allowed to acclimatize for 1 week. Animals were maintained under specified pathogen-free conditions at the Animal Resource Center at 24 ± 2 °C with 30–70% humidity and a 12-h alternating light–dark cycle. Animals were housed six/cage and given sterilized food and autoclaved water *ad libitum*. Guidelines for the humane treatment of animals were followed as approved by the Animal Care and Use Committee.

Subconfluent monolayers of human colon carcinoma cells (HT29) were harvested and resuspended in PBS, containing no supplements, and subcutaneously implanted (5×10^5–1×10^6 cells in 100 µl of PBS) on the backs of the mice. The animals were observed daily until the tumors became visible, after which the tumors were measured three times a week in two perpendicular dimensions using a digital caliper. The tumor weight was calculated following the equation: weight $= 1/2 \cdot a^2 \cdot b$, where *a* and *b* are the smaller and the larger diameters, respectively. When the median tumor size reached 100–400 mg, *staging day*, the animals were randomized into treatment groups (six animals/group). The treatment schedule consisted of one cycle (q4 × 3d, on days 1, 5, and 9) of i.v. administration of free DOX or L-DOX (4 mg/kg) or the equivalent lipid or peptide content of each preparation and adjusted based on animal weight determined at the time of treatment. The mice were weighed every day for the first 2 weeks after treatment and three times a week thereafter. The death of a mouse within 2 weeks after the final injection was considered as toxic death and the animal was excluded from further calculations. When the tumor grew to a size beyond possible regression (5 g), the mouse was euthanized and this day was computed for survival calculations. GraphPad software was used for analyzing the *in vivo* tumor growth, using the Gompertz function for data fitting and the two-way analysis of variance (ANOVA) for comparing curves.

Data Analysis

Each experiment was performed at least three times, with each data point performed in triplicate. Results are expressed as mean ± SEM. Most comparisons were performed with the Student's *t*-test for unpaired data.

Results

Preparation of Liposomes

Liposomal composition was selected according to previous studies [16]. PC and NGPE were saturated, and PG was from natural sources. Saturated phospholipids are chemically and physically more stable than unsaturated ones and bilayers are rigid at body temperatures. The presence of PG was decided in order to confer a negative charge to the vesicles' surface that could be beneficial to avoid vesicles' aggregation and to reduce the potential release of protonated DOX. Chol content was a little bit higher than usual to compensate the motion of unsaturated PG chains. Although extrusion through polycarbonate filters renders more homogeneous preparations than sonication, this was the method of choice in order to avoid excessive manipulation of the samples that could result in contamination and lose of components. For similar reasons, dialysis was preferred instead of size exclusion chromatography because with this last technique a certain level of dilution cannot be avoided. Final CTRs of size and polydispersity indicated that these values increased softly after reaction but still remain clearly under 200 nm that was the requirement for *in vivo* administration.

Yields on DOX encapsulation were around 80%. The amount of peptide linked to the surface of liposomes represented a 60% of

Table 1. Attachment of endothelial and tumor cells to immobilized peptides

	HUVEC	HT29
TSP_1-B	289.70 ± 84.2[a]	2.36 ± 2.7[b]
[Abu6]TSPB	181.80 ± 41.4	71.34 ± 17.4
TSP_2-A	105.20 ± 20.0	27.89 ± 15.4[b]
[Abu6]TSPA	125.60 ± 28.8	118.20 ± 24.7
TSP_1	100	100

Data are the mean ± SEM of the percentage of cell attachment with respect to the cell adhesion on TSP-1 (20 μg/ml).
[a] $P < 0.05$.
[b] $P < 0.0005$.

the available reactive NGPE terminal carboxyl ends. These results were in agreement to a previous systematic study carried out with the same type of liposomes [16]. Besides, physicochemical interactions between peptides and lipids were performed, and the results indicate that these peptides have low affinity for lipids. This confirms indirectly that the peptide content quantified by amino acid analyses corresponds to peptide chains linked to the surface of vesicles.

Peptide Sequences Mediate the Adhesion of Tumor and Endothelial Cells

In order to select those sequences able to support the adhesion of both types of cells, as a first approach, we compared the attachment of tumor and endothelial cells on 0.25 μM immobilized peptides: TSP_1-B and TSP_2-A (natural peptides) and [Abu6]TSPB and [Abu6]TSPA (aspartimide analogs). Table 1 shows that the aspartimide analogs were better ligands for tumor cells than the natural peptides and, at the peptide concentration used, the attachment of tumor and endothelial cells to [Abu6]TSPA was similar to the attachment on 20 μg/ml of TSP-1.

Subsequently, increasing amounts of [Abu6]TSPB and [Abu6]TSPA were immobilized on microtiter plate wells and the attachment of endothelial and tumor cells was measured and compared with the cell adhesion on TSP-1 (20 μg/ml). As shown in Figure 1A and B, HUVEC adhesion increased with the peptide concentration and it was higher on [Abu6]TSPB than on [Abu6]TSPA, suggesting that endothelial cells differentiate between TSP-1- and TSP-2-derived sequences. However, HT29 cells attached better on [Abu6]TSPA and, between 0.1 and 0.3 mM, tumor and endothelial cells adhered similarly to this peptide. Finally, we selected [Abu6]TSPB and [Abu6]TSPA as potential tools for liposome targeting.

Effect of Peptides on HUVEC and Tumor Cell Proliferation

Given that cell proliferation is required in angiogenesis, tumor progression, and invasion, the effect of aspartimide analogs on the endothelial and tumor cell proliferation was measured. To this end, HUVE and HT29 cells were cultured for 72 h in the presence of increasing concentrations of [Abu6]TSPB and [Abu6]TSPA as described in Materials and Methods Section. Both peptides increased the proliferation of endothelial cells, but this effect started at lower concentrations and reached a higher plateau with [Abu6]TSPB than with [Abu6]TSPA (Figure 2A). At the concentration range used in this study, [Abu6]TSPB but not [Abu6]TSPA slightly increased the *in vitro* proliferation of HT29 human carcinoma cells (Figure 2B).

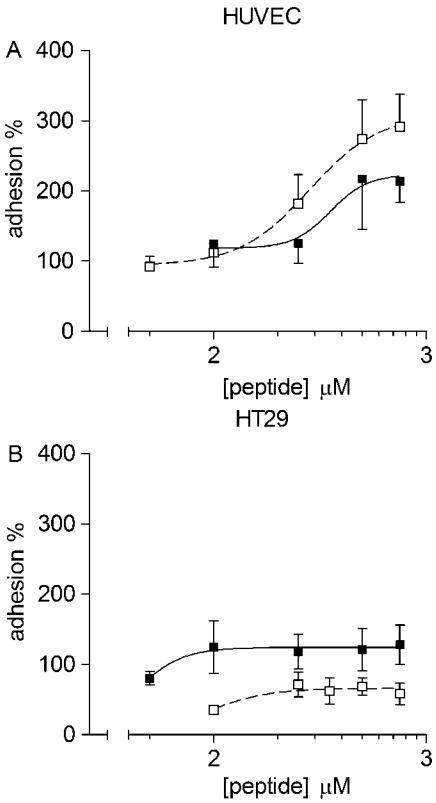

Figure 1. Attachment of tumor and endothelial cells on [Abu6]TSPA and [ABU6]TSPB. Peptide sequences were coated overnight on flat clear bottom, black 96-well plates. Cells (1×10^5/100 μl) labeled with (5 μM) Calcein-AM were added to each well and after 45-min incubation at 37 °C in a humidified atmosphere (5% CO_2), the fluorescence was measured (485/535 filters). The cell adhesion was calculated as a percentage of corrected (background subtracted) fluorescence of peptide-coated wells with respect to that measured in TSP-1 coated wells (20 μg/ml). Data are depicted as mean ± SE of three separate experiments.

Influence of [Abu6]TSPB and [Abu6]TSPA on Angiogenesis

The effect of the peptide sequences on the HUVEC tube formation on Matrigel is shown in Figure 3A. Tube formation increased when HUVECs were grown in the presence of 0.2 mM [Abu6]TSPB ($P = 0.025$) and was not significantly altered by [Abu6]TSPA (0.3 m M).

Furthermore, the effect of peptides on *in vivo* angiogenesis by CAM assay was evaluated. Upon dissection of the CAM of a 10-day-old chick embryo, the spontaneous angiogenesis in CAM was clearly observed. After its topical application for 48 h, [Abu6]TSPB showed no effect on the new vessel formation (Figure 3B). However, [Abu6]TSPA significantly inhibited the spontaneous angiogenesis when compared with CTR untreated CAM ($P < 0.0005$), or with FGF-b-treated CAM ($P = 0.0002$). Therefore, despite its slight increase in endothelial cell proliferation, [Abu6]TSPA is an effective inhibitor of angiogenesis *in vivo*.

HT29 Tumor Growth Evolution in Mice Treated with Peptide-Targeted Liposomes

Five-week-old male nu/nu Swiss mice were randomized into treatment groups: (i) free DOX, (ii) doxorubicin encapsulated in a peptide-free L-DOX, (iii) DOX encapsulated in a peptide-targeted liposome: (L-DOX-[Abu6]TSPB or L-DOX-[Abu6]TSPA), (iv) peptide-targeted liposome without DOX: (L-[Abu6]TSPB or L-[Abu6]TSPA),

Journal of PeptideScience

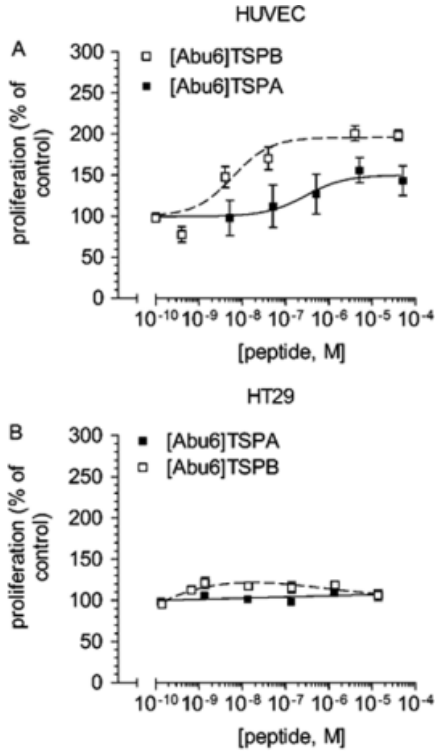

Figure 2. Effect of peptides on HUVEC and tumor cells proliferation. Dose–response curves of HUVEC (A) and HT29 (B) cells after 72-h exposure to increasing concentrations of [Abu6]TSPB and [Abu6]TSPA (mean ± SEM of 4–6 experiments). Cells were plated as described in methods and 24 h later, the cells were refed with 10% FBS-supplemented culture medium containing increasing concentrations of peptide. Proliferation is expressed as the percentage of control (excipient treated) cultures and GraphPad software was used for the cell-growth curves' fitting.

and (v) vehicle (CTR). The treatment consisted of one cycle, q4 × 3d, on days 1, 5, and 9 of i.v. administration of 4 mg/kg of either-free DOX or L-DOX, or the equivalent lipid and peptide content of each preparation, and adjusted on the basis of animal weight determined at the time of treatment. CTR groups were scheduled simultaneously with individual testing groups.

The tumor growth with time in animals treated with DOX and L-DOX was similar, and not significantly different from the CTR group (data not shown), showing that in our experimental conditions, DOX is scarcely active on HT29 carcinoma. Besides, neither L-[Abu6]TSPA- nor L-[Abu6]TSPB-targeted liposomes without DOX significantly modify the tumor growth evolution in mice (data not shown).

The treatment of tumor-bearing mice with peptide-targeted L-DOX (i.v. 4 mg/kg of DOX) resulted in different tumor growth evolution depending on the peptide sequence used. L-DOX-[Abu6]TSPA significantly reduced the tumor growth rate ($P > 0.0001$), which was measured using the Gompertz equation (Figure 4A). However, the mice treated with L-DOX-[Abu6]TSPB liposomes had a tumor evolution even slightly worse than that of CTRs (Figure 4B). Given that peptide equivalent doses of L-[Abu6]TSPA had no effect on tumor growth, we assume that the therapeutic effect measured in L-DOX-[Abu6]TSPA-treated mice should be mainly attributed to the cytotoxic effect of DOX.

Survival curves agree with these results, showing that a single cycle of treatment with L-DOX-[Abu6]TSPA increased the life span of the tumor-bearing mice by 58% ($P < 0.008$), whereas the survival of L-[Abu6]TSPA-treated mice was similar to that of the CTR group (Figure 5A). However, the administration of equivalent doses of L-DOX-[Abu6]TSPB or L-[Abu6]TSPB had a toxic effect on mice, and those animals surviving the treatment had a tumor evolution similar to that of CTR animals (Figure 5B). As expected, neither 4 mg/kg of DOX nor L-DOX had any effect on the survival time of the tumor-bearing mice (data not shown).

Discussion

In this study, we show that L-DOX with [Abu6]TSPA, the aspartimide analog of a TSR TSP_1-A incorporated at the lipid bilayer, exerts tumor growth-inhibiting effects *in vivo*. This DOX formulation was effective in the treatment of colorectal carcinoma when administered in a single cycle dosing schedule at lower doses than those required for free DOX.

The therapeutic effect of L-DOX-[Abu6]TSPA should be mainly attributed to the cytotoxic effect of DOX given that equivalent doses of L-[Abu6]TSPA (DOX-free liposomes) had no effect on tumor growth. However, the slight increase in endothelial cell proliferation produced by [Abu6]TSPA inserted on the L-DOX could facilitate the cytotoxic effect of the anthracycline.

Nevertheless, some involvement of the antiangiogenic effect of [Abu6]TSPA cannot be overlooked, especially given the lack of antitumor effect of L-DOX bearing [Abu6]TSPB as vector peptide.

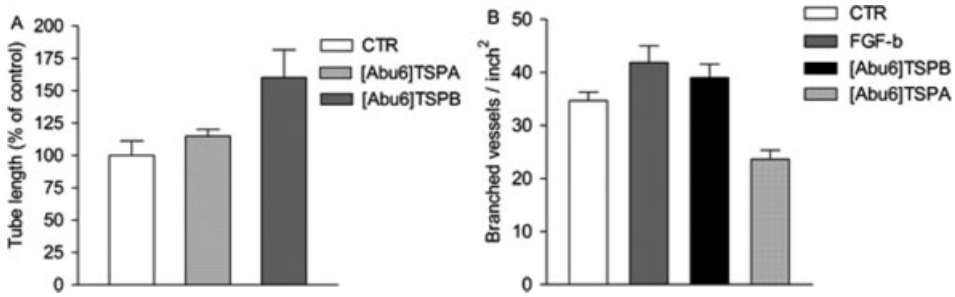

Figure 3. Influence of [Abu6]TSPB and [Abu6]TSPA on angiogenesis. (A) Tube formation of HUVECs on Matrigel after 24 h of cell seeding. Sprouting and tubulogenesis were observed under an inverted phase-contrast microscope and photographed. Images were scanned and tube length was measured using Scion Image software. Data are reported as tube length percentage of control (CTR; data are mean ± SEM of 2–4 experiments). (B) Spontaneous angiogenesis in the CAM assay after topical application of peptides for 48 h. Areas containing only capillary plexus were selected for quantification and at least four and up to ten such areas per micrograph were identified. Digital images of the CAM were captured using a binocular dissection microscope and angiogenesis quantification was done with Scion Image software measuring the number of branched vessels per area. Data are reported as percentage of CTR (mean ± SEM).

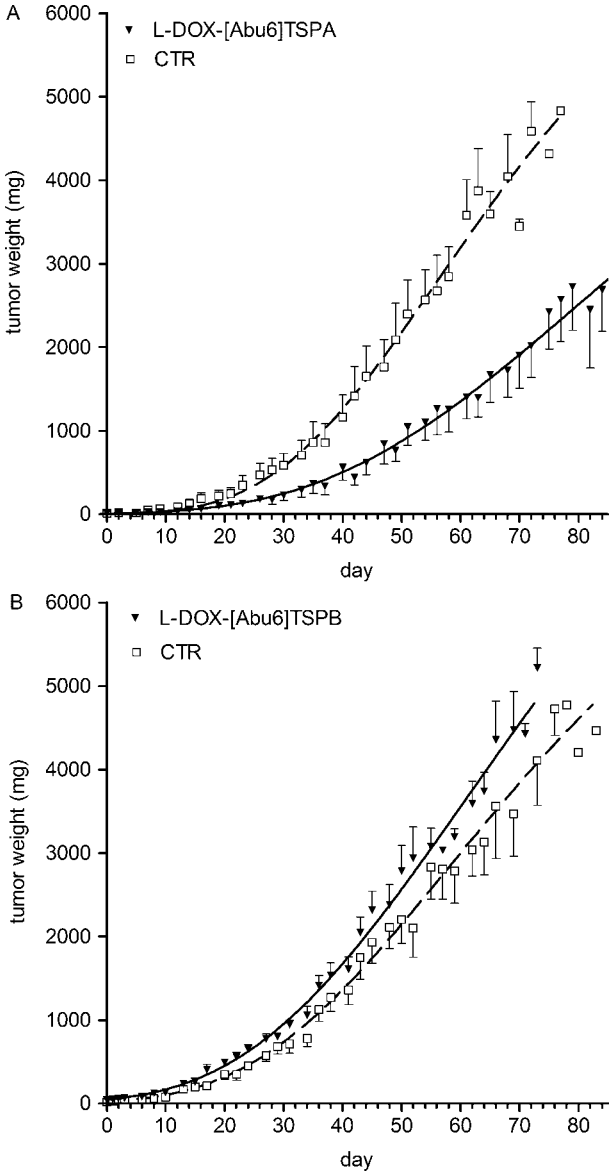

Figure 4. HT29 tumor growth evolution in mice treated with peptide-targeted L-DOX. Cells were subcutaneously implanted on the back of the mice as described in Materials and Methods Section. At the *staging day*, animals were randomized into various groups (six animals/group) and treated: one cycle, q4 × 3d, on days 1, 5, and 9 of i.v. administration of: (A) L-DOX-[Abu6]TSPA and (B) L-DOX-[Abu6]TSPB liposomes (4 mg/kg DOX). L-DOX-[Abu6]TSPA significantly reduced the tumor growth rate ($P > 0.0001$). Control groups were scheduled simultaneously with individual testing groups. Gompertz function was used for data fitting and the two-way ANOVA for comparing curves.

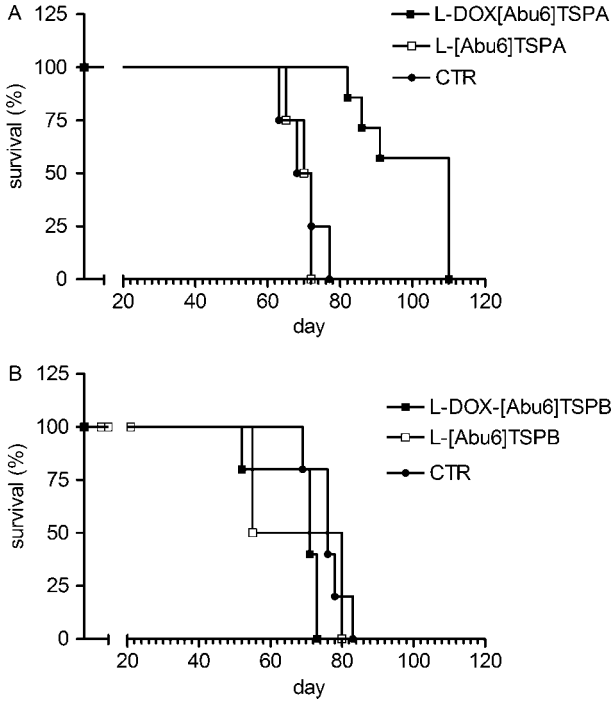

Figure 5. Survival curves of tumor-bearing mice. Mice were treated with peptide-targeted liposomes loaded or not with DOX and containing (A) [Abu6]TSPA and (B) [Abu6]TSPB conjugated to the lipid bilayer surface. The treatment schedule consisted of one cycle, q4 × 3d, on days 1, 5, and 9 of i.v. administration of 4 mg/kg DOX, or the equivalent lipid and peptide content of each preparation, and adjusted on the basis of animal weight determined at the time of treatment. Control (CTR) groups were scheduled simultaneously with individual testing groups. Tumor volume was measured three times weekly until it reached 5 g; at this time, the animal was sacrificed for humane reasons and this day was computed for survival calculations. $P = 0.04$ for L-DOX-[Abu6]TSPA with respect to CTR group.

We have shown that, despite the slight increase in endothelial cells' proliferation due to [Abu6]TSPA, this peptide is an effective inhibitor of angiogenesis *in vivo* (spontaneous angiogenesis in CAM assay). In contrast, although [Abu6]TSPB is also a good ligand for tumor and endothelial cells, it considerably increases endothelial cell proliferation, tube formation, and spontaneous angiogenesis in CAM assay, and when incorporated at the liposome surface, it results in a higher toxicity and null effect on tumor growth. Thus, we consider that the antiangiogenic effect of [Abu6]TSPA could also contribute to the antitumor action of L-DOX-[Abu6]TSPA liposomes, although the low levels of peptide incorporated to L-[Abu6]TSPA liposome surface were not enough by themselves to induce tumor regression.

In summary, data reported here are promising because they show that the *in vivo* antitumor effect of L-DOX increases with the incorporation of a peptide vector that recognizes tumor and endothelial cells. The effect is dependent on the antiangiogenic action of the peptide vector used, given that no antitumor effect was produced when [Abu6]TSPB was used for vectorization of the liposomes. We believe that adjusting the DOX dosage and schedule could increase the therapeutic effect attained, probably taking advantage of the antiangiogenic effect induced by the metronomic dosage of the anthracycline [18,19].

Acknowledgements

This work was supported by the Spanish Ministry of Science and Technology, Grant No. PTR1995-0596-OP.

References

1 Eberhard A, Kahlert E, Goede V, Hemmerlein B, Plate KH, Augustin HG. Heterogeneity of angiogenesis and blood vessel maturation in human tumors: implications for antiangiogenic tumor therapies. *Cancer Res.* 2000; **60**: 1388–1393.
2 Hahnfeldt P, Panigrahy D, Folkman J, Hlatky L. Tumor development under angiogenic signaling: a dinamical theory of tumor growth,

Journal of PeptideScience

treatment response, and postvascular dormancy. *Cancer Res.* 1999; **59**: 4770–4775.
3 Corti A, Ponzoni M. Tumor vascular targeting with tumor necrosis factor alpha and chemotherapeutic drugs. *Ann. N Y Acad. Sci.* 2004; **1028**: 104–112.
4 Maeda N, Takeuchi Y, Takada M, Sadzuka Y, Namba Y, Oku N. Anti-neovascular therapy by use of tumor neovasculature-targeted long-circulating liposome. *J. Control. Release* 2004; **100**: 41–52.
5 Pastorino F, Brignole C, Marimpietri D. Vascular damage and anti-angiogenic effects of tumor vessel-targeted liposomal chemotherapy. *Cancer Res.* 2003; **63**: 7400–7409.
6 Chen H, Herndon ME, Lawler J. The cell biology of thrombospondin-1. *Matrix Biol.* 2000; **19**: 597–614.
7 Guo N-H, Krutzsch HC, Inman JK, Roberts DD. Thrombospondin 1 and type 1 repeat peptides of thrombospondin 1 specifically induce apoptosis of endothelial cells. *Cancer Res.* 1997; **57**: 1735–1742.
8 Iruela-Arispe ML, Lombardo M, Krutzsch HC, Lawler J, Roberts DD. Inhibition of angiogenesis by thrombospondin-1 is mediated by two independent regions within the type 1 repeats. *Circulation* 1999; **100**: 1423–1431.
9 Murphy-Ullrich JE, Poczatec M. Activation of latent TGF-β by thrombospondin-1: mechanisms and physiology. *Cytokine Growth Factor Rew.* 2000; **11**: 59–69.
10 Schultz-Cherry S, Chen J, Mosher DF, Misenheimer TM, Krutzsch HC, Roberts DD, Murphy-Ullrich JE. Regulation of transforming growth factor-β activation by discrete sequences of thrombospondin 1. *J. Biol. Chem.* 1995; **270**: 7304–7310.
11 Guo NH, Krutzsch HC, Inman JK, Shannon CS, Roberts DD. Antiproliferative and antitumor activities of D-reverse peptides derived from the second type-1 repeat of thrombospondin 1. *J. Pept. Res.* 1997; **50**: 210–221.
12 Cebrian J, Grau-Oliete MR, Rivera-Fillat MP, Reig F. Synthesis and biological activity of thrombospondin related peptides. *Curr. Topics Pept. Protein Res.* 2001; **4**: 81–88.
13 Cebrián J, Domingo V, Reig F. Synthesis of peptide sequences related to thrombospondin: factors affecting aspartimide by-product formation. *J. Pept. Res.* 2003; **62**: 238–244.
14 Bogdanov AA Jr, Klibanov AL, Torchilin VP. Protein immobilization on the surface of liposomes via carbodiimide in presence of *N*-hydroxysulfosuccinimide. *FEBS Lett.* 1988; **231**: 381–384.
15 Casas J, Gorchs F, Sánchez-Baeza P, Teixidor P, Messeguer A. Inhibition of rat liver microsomal lipid peroxidation elicited by simple 2,2-dimethylcromenes and chromans structurally related to precocenes. *J. Agric. Food Chem.* 1992; **40**: 585–590.
16 Almiñana N, Polo D, Rodriguez L, Reig F. Biodistribution study of doxorubicin encapsulated in liposomes: influence of peptide coating and lipid composition. *Prep. Biochem. Biotech.* 2004; **34**: 77–96.
17 Skehan P, Storneg R, Scudiero D, Monks A, McMahon J, Vistica D, Warren JT, Bokesch H, Kenney S, Boyd MR. New colorimetric cytotoxicity assay for anticancer-drug screening. *J. Natl. Cancer Inst.* 1990; **82**: 1107–1112.
18 Hanahan D, Bergers G, Bergsland E. Less is more, regularly metronomic dosing of cytotoxic drugs can target tumor angiogenesis in mice. *J. Clin. Invest.* 2000; **105**: 1047–7.
19 Lennernäs B, Albertsson P, Lennernäs H, Norrby K. Chemotherapy and antiangiogenesis. Drug-specific, dose-related effects. *Acta Oncol.* 2003; **42**: 294–303.

